

## Supported Catalysts

International Edition: DOI: 10.1002/anie.201604673  
German Edition: DOI: 10.1002/ange.201604673

# Co<sub>3</sub>O<sub>4</sub> Nanoparticles Supported on Mesoporous Carbon for Selective Transfer Hydrogenation of $\alpha,\beta$ -Unsaturated Aldehydes

Guang-Hui Wang, Xiaohui Deng, Dong Gu, Kun Chen, Harun Tüysüz, Bernd Spliethoff, Hans-Josef Bongard, Claudia Weidenthaler, Wolfgang Schmidt, and Ferdi Schüth\*

Dedicated to Professor Klaus K. Unger on the occasion of his 80th birthday

**Abstract:** A simple and scalable method for synthesizing Co<sub>3</sub>O<sub>4</sub> nanoparticles supported on the framework of mesoporous carbon (MC) was developed. Benefiting from an ion-exchange process during the preparation, the cobalt precursor is introduced into a mesostructured polymer framework that results in Co<sub>3</sub>O<sub>4</sub> nanoparticles (ca. 3 nm) supported on MC (Co<sub>3</sub>O<sub>4</sub>/MC) with narrow particle size distribution and homogeneous dispersion after simple reduction/pyrolysis and mild oxidation steps. The as-obtained Co<sub>3</sub>O<sub>4</sub>/MC is a highly efficient catalyst for transfer hydrogenation of  $\alpha,\beta$ -unsaturated aldehydes. Selectivities towards unsaturated alcohols are always higher than 95 % at full conversion. In addition, the Co<sub>3</sub>O<sub>4</sub>/MC shows high stability under the reaction conditions, it can be recycled at least six times without loss of activity.

The production of high-value-added chemicals from biomass is of major interest since the dependence on petroleum-based chemicals can be reduced by replacing fossil feedstocks with renewable ones.<sup>[1]</sup> Furan derivatives of furfural (FAL) and 5-hydroxymethylfurfural (HMF), which can be produced from hemicellulose and cellulose, respectively, are considered as promising platform molecules to bridge the gap between biomass resources and bio-chemicals, since they can be converted into a variety of high-value-added chemicals and fuels.<sup>[2]</sup> Particularly, selective hydrogenation of FAL to furfuryl alcohol (FOL) and HMF to 2,5-bis-(hydroxymethyl)-furan (BHMF) has great potential for industrial applications. Because, FOL and BHMF can be used as precursors in the synthesis of polymers, resins and adhesives, and as intermediates for the generation of drugs and crown ethers.<sup>[1c,f]</sup> However, owing to the different functionalities of furan-based  $\alpha,\beta$ -unsaturated aldehydes (e.g., furan ring, C=C and C=O bonds),<sup>[3]</sup> selective hydrogenation of only the C=O bond is very challenging. Many byproducts are often formed by hydrogenolysis of the -CH=O side chain to -CH<sub>3</sub>, or hydrogenation of the furan ring and its opening,<sup>[4]</sup> leading to low yield of the desired unsaturated alcohols and increasing costs

for product purification. Therefore, design of suitable catalysts and/or catalytic systems that facilitate selective hydrogenation of C=O bond in the presence of other functionalities is highly desirable.

In general, conventional hydrogenation catalysts based on transition metals (e.g., Pd, Pt, Ru, Rh, Cu, or Ni) show high activity but poor selectivity toward unsaturated alcohols.<sup>[4,5]</sup> To enhance the selectivity for unsaturated alcohols over such catalysts, additives,<sup>[6]</sup> stabilizers/ligands,<sup>[7]</sup> supplemental metal components,<sup>[8]</sup> and functional supports<sup>[9]</sup> were introduced into catalytic systems or catalysts. In some cases high selectivity toward unsaturated alcohols and high activity were indeed achieved using the above approaches. However, owing to the complexity of reaction mechanisms (e.g., competitive/non-competitive and dissociative/non-dissociative adsorption, side reactions), selectivities and activities in these cases can be affected by a series of factors, including the structure, texture and composition of the catalysts (e.g., particle size, shape, molar ratio of different components, crystal structure) and the reaction conditions (e.g., temperature, pressure and solvent).<sup>[10]</sup> In other words, dramatic decrease in selectivity and/or activity often occurs, because it is very difficult to predict and control the influence of these factors precisely, especially in large scale applications. Therefore, it is necessary to develop simple methods for scale-up of catalyst synthesis. Furthermore, the catalysts must be highly active and selective toward unsaturated alcohols in simple catalytic systems, which are also controllable and scalable.

Compared with hydrogenation reactions involving H<sub>2</sub>, transfer hydrogenation is much safer and easier to handle because pressure is not an issue and the influence of H<sub>2</sub> pressure on selectivity is not relevant.<sup>[11]</sup> In transfer hydrogenation reactions, 2-propanol is often utilized as hydrogen donor, because it is cheap, environmentally friendly, and easy to remove.<sup>[11]</sup> Herein, we report on the transfer hydrogenation of furan-based  $\alpha,\beta$ -unsaturated aldehydes over spinel-type cobalt oxide on mesoporous carbon (Co<sub>3</sub>O<sub>4</sub>/MC), where the selectivity toward unsaturated alcohol is always higher than 95 % at full conversion. The synthesis of Co<sub>3</sub>O<sub>4</sub>/MC involves a hydrothermal process, an ion-exchange, and a pyrolysis/reduction as well as a mild oxidation step (Figure 1 a). In the first step, a mesostructured polymer gel is synthesized using 2,4-dihydroxybenzoic acid and hexamethylenetetramine (HMT) as polymer precursors, and triblock copolymer (P123) as surfactant under hydrothermal conditions (130 °C for 4 h). Then, cobalt ammine complexes are introduced

\* Dr. G.-H. Wang, X. Deng, Dr. D. Gu, Dr. K. Chen, Dr. H. Tüysüz, B. Spliethoff, H.-J. Bongard, Dr. C. Weidenthaler, Dr. W. Schmidt, Prof. Dr. F. Schüth  
Max-Planck-Institut für Kohlenforschung  
45470 Mülheim an der Ruhr (Germany)  
E-mail: schueth@mpi-muelheim.mpg.de

Supporting information for this article can be found under:  
<http://dx.doi.org/10.1002/anie.201604673>.

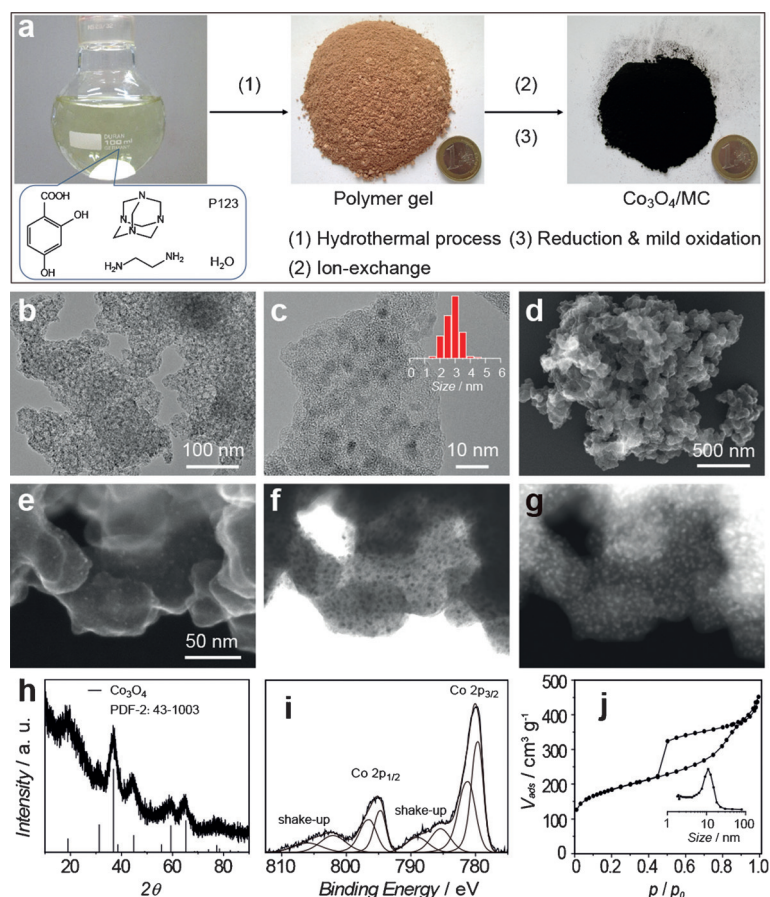


**Figure 1.** a) Synthesis of  $\text{Co}_3\text{O}_4/\text{MC}$ . b,c) TEM images, d) SEM image and e–g) STEM images of  $\text{Co}_3\text{O}_4/\text{MC}$ ; inset in (c) shows the  $\text{Co}_3\text{O}_4$  particle size distribution. h) XRD pattern, i) XPS spectrum, and j)  $\text{N}_2$  sorption isotherm of  $\text{Co}_3\text{O}_4/\text{MC}$ ; inset: the pore size distribution.

homogenously into the polymer framework via ion exchange. Next, the polymer containing the cobalt precursor is pyrolyzed at  $500^\circ\text{C}$  (10%  $\text{H}_2$  in argon) to form the carbon, simultaneously the cobalt precursor is reduced to form metal nanoparticles supported on the mesopore framework of the carbon. Finally,  $\text{Co}_3\text{O}_4$  nanoparticles are formed within the MC support after mild oxidation at room temperature (1%  $\text{O}_2$  in argon). These synthetic processes can be easily scaled up.

Transmission electron microscopy (TEM) images (Figure 1b,c) show that the  $\text{Co}_3\text{O}_4/\text{MC}$  is highly mesoporous. The  $\text{Co}_3\text{O}_4$  nanoparticles with a diameter of approximately 3 nm are finely dispersed on the framework of MC. Many macropores are also observed in the scanning electron microscopy (SEM) images (Figure 1d and Figure S1a in the Supporting Information), which are caused by the gel structure of the polymer. Scanning transmission electron microscopy (STEM) images (Figure 1e–g) further confirm that the  $\text{Co}_3\text{O}_4$  nanoparticles are very homogeneously dispersed on the MC framework and that they have a narrow particle size distribution. Most importantly, no bigger  $\text{Co}_3\text{O}_4$  particles are formed by the synthesis method (Figure 1b,e–g and Figure S1b). The X-ray diffraction (XRD) pattern (Figure 1h) shows the typical reflections of the  $\text{Co}_3\text{O}_4$  spinel (the lines

under the diffraction pattern indicate reflections for the PDF-2 entry 43–1003). The very broad reflections prove the formation of small  $\text{Co}_3\text{O}_4$  nanoparticles after the reduction and mild oxidation steps. The Co 2p X-ray photoelectron spectrum (XPS) shows peaks with binding energies at 779.6 eV and 794.6 eV corresponding to  $\text{Co}^{3+} 2p_{3/2}$  and  $2p_{1/2}$ , and peaks at 781.1 eV and 796.5 eV belonging to  $\text{Co}^{2+} 2p_{3/2}$  and  $2p_{1/2}$  (Figure 1i, Table S1), which further confirm the formation of  $\text{Co}_3\text{O}_4$  nanoparticles. Nevertheless, the shake-up signal at 785.4 eV belonging to  $\text{Co}^{2+}$  is slightly higher than expected for an ideal  $\text{Co}_3\text{O}_4$  surface, suggesting that  $\text{Co}^{2+}$  is enriched in the surface of the  $\text{Co}_3\text{O}_4$  nanoparticles (Figure 1i, Table S1). Based on AAS analysis (atomic absorption spectrometry, PerkinElmer AAnalyst 200), the Co fraction in  $\text{Co}_3\text{O}_4/\text{MC}$  is 15 wt %, corresponding to 20 wt %  $\text{Co}_3\text{O}_4$ . The  $\text{N}_2$  sorption isotherm of  $\text{Co}_3\text{O}_4/\text{MC}$  (Figure 1j) shows a type-IV curve, characteristic for mesoporous materials. The sorption isotherm does not level out in a plateau at relative pressures  $p/p_0 > 0.9$ , indicating the existence of macropores, fully consistent with the SEM observations. The surface area, pore volume and pore size of  $\text{Co}_3\text{O}_4/\text{MC}$  are  $642 \text{ m}^2 \text{ g}^{-1}$ ,  $0.7 \text{ cm}^3 \text{ g}^{-1}$  and 11 nm, respectively.

The synthesis methodology of  $\text{Co}_3\text{O}_4/\text{MC}$  can be extended to synthesize other metal catalysts supported on MC. Pd/MC (Figure S2) and Ru/MC (Figure S3) were prepared by this method as well, both of which have narrow particle size distribution ( $5 \pm 0.8 \text{ nm}$  for Pd;  $1 \pm 0.2 \text{ nm}$  for Ru) and homogenous dispersion. Without introducing metals, MC with a surface area of  $722 \text{ m}^2 \text{ g}^{-1}$ , a pore volume of  $0.7 \text{ cm}^3 \text{ g}^{-1}$  and a pore size of around 9.5 nm is generated directly after carbonization of the polymer gel at  $800^\circ\text{C}$  in argon (Figure S4). Such carbon material has high potential for applications as catalyst support or adsorbent.

The catalytic performance of  $\text{Co}_3\text{O}_4/\text{MC}$  was evaluated for transfer hydrogenation of FAL to FOL and HMF to BHMF. First a blank reaction without catalyst was carried out; no reaction proceeded (Table S2, entry 1). In the presence of pure MC, the conversion of FAL was lower than 4% after reaction for 8 h at  $120^\circ\text{C}$  (Table S2, entry 2). However, when using  $\text{Co}_3\text{O}_4/\text{MC}$  as catalyst, full conversion of FAL into FOL (selectivity  $> 97\%$ ) was achieved after reaction for 8 h at  $120^\circ\text{C}$  (Figure 2a). Also, a 97% selectivity of BHMF at complete conversion of HMF was realized within 48 h at  $120^\circ\text{C}$  (Figure 2b). In both cases, only trace amounts of byproducts ( $< 3\%$ ) generated from the aldol condensation of substrates and acetone were observed. Undesired saturated aldehydes and saturated alcohols were not observed by GC-MS (detection threshold 0.3%), indicating that  $\text{Co}_3\text{O}_4/\text{MC}$  is a truly selective hydrogenation catalyst for the  $\text{C}=\text{O}$  bond. Extending the reaction time for FAL hydrogenation to 24 h, the selectivity towards FOL was unchanged (Figure 2a), further confirming that the  $\text{C}=\text{C}$  bond is unaffected under the reaction conditions. It is unclear whether the surface under

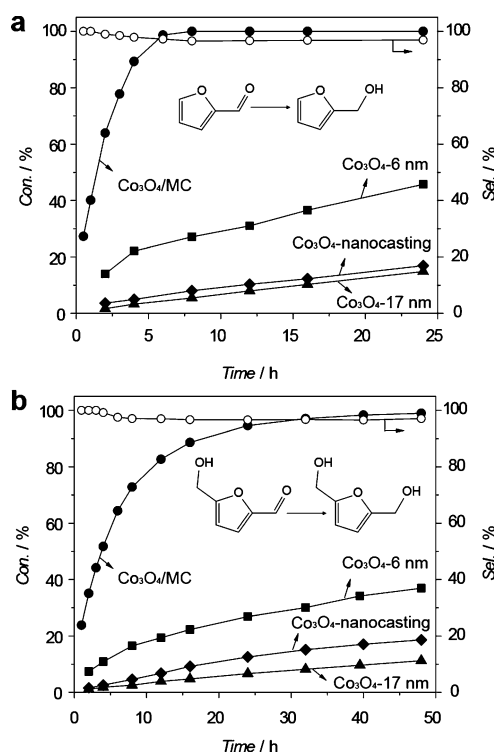


**Figure 2.** Catalytic performance in transfer hydrogenation reactions at 120°C: a) FAL to FOL and b) HMF to BHMF over  $\text{Co}_3\text{O}_4/\text{MC}$ ,  $\text{Co}_3\text{O}_4$ -nanocasting,  $\text{Co}_3\text{O}_4$ -6 nm, and  $\text{Co}_3\text{O}_4$ -17 nm. Reaction conditions: 1 mmol substrate, 10 mL 2-propanol, 50 mg  $\text{Co}_3\text{O}_4/\text{MC}$ , 25 mg for  $\text{Co}_3\text{O}_4$ -nanocasting,  $\text{Co}_3\text{O}_4$ -6 nm, and  $\text{Co}_3\text{O}_4$ -17 nm, respectively.

reaction conditions consists of  $\text{Co}_3\text{O}_4$  or somewhat reduced species. The presence of metallic cobalt, however, is highly improbable, since comparison experiments using the materials prior to the final oxidation step resulted in a much inferior activity (Figure S6).

For comparison, mesoporous  $\text{Co}_3\text{O}_4$  synthesized by nanocasting ( $\text{Co}_3\text{O}_4$ -nanocasting, Figure S5a,b)<sup>[12]</sup> was used as catalyst in the same system. The activity of  $\text{Co}_3\text{O}_4$ -nanocasting was much lower than that of  $\text{Co}_3\text{O}_4/\text{MC}$ . Conversions of FAL and HMF were only 17% and 19% after reaction for 24 h and 48 h, respectively (Figure 2a,b). From the XRD pattern of  $\text{Co}_3\text{O}_4$ -nanocasting one can infer, that its crystalline domain sizes are bigger than those of  $\text{Co}_3\text{O}_4/\text{MC}$  (Figure S5b). Furthermore,  $\text{Co}_3\text{O}_4$  nanoparticles with different sizes (6 nm and 17 nm) synthesized by a reported preparation method without any surfactants (Figure S5c–f)<sup>[13]</sup> were also tested. The conversions of FAL over  $\text{Co}_3\text{O}_4$ -6 nm and  $\text{Co}_3\text{O}_4$ -17 nm were 46% and 15% within 24 h, indicating that smaller  $\text{Co}_3\text{O}_4$  nanoparticles show higher activity (Figure 2a). Similar results were found for the transfer hydrogenation of HMF, the  $\text{Co}_3\text{O}_4$ -6 nm shows higher activity (Figure 2b). In all cases, the selectivities for FOL and BHMF were always higher than 97% (Table S2, entries 6–8, 12–14), indicating that the selectivity over  $\text{Co}_3\text{O}_4$  is structure insensitive.

The surface area of  $\text{Co}_3\text{O}_4$  nanoparticles, assumed to be spherical, is used to normalize the reaction rate for FAL conversion. Basing the normalization on surface areas determined by nitrogen sorption for both pure samples

gives essentially identical results. The rates (calculated based on the conversion reached over a certain period of time selected so that conversion over different catalysts were approximately identical) over  $\text{Co}_3\text{O}_4$ -6 nm and  $\text{Co}_3\text{O}_4$ -17 nm are  $14.0 \times 10^{-3}$  (22% conversion in 4 h) and  $4.5 \times 10^{-3} \text{ mmol m}_{\text{Co}_3\text{O}_4}^{-2} \text{ h}^{-1}$  (15% conversion in 24 h; Table S2, entries 7,8), respectively. For HMF conversion, the reaction rates over  $\text{Co}_3\text{O}_4$ -6 nm and  $\text{Co}_3\text{O}_4$ -17 nm are  $4.0 \times 10^{-3}$  (19% conversion in 12 h) and  $1.7 \times 10^{-3} \text{ mmol m}_{\text{Co}_3\text{O}_4}^{-2} \text{ h}^{-1}$  (11% conversion in 48 h; Table S2, entries 13, 14), respectively. Thus, intrinsic activities of the smaller particles seem to be by about a factor of three higher. Surprisingly, the reaction rates for FAL and HMF conversions over  $\text{Co}_3\text{O}_4/\text{MC}$  are  $114.5 \times 10^{-3}$  (64% conversion in 2 h) and  $33.9 \times 10^{-3} \text{ mmol m}_{\text{Co}_3\text{O}_4}^{-2} \text{ h}^{-1}$  (64% conversion in 6 h; Table S2, entries 3,9), respectively, which are much higher than those over unsupported  $\text{Co}_3\text{O}_4$  nanoparticles. This suggests a synergistic effect between  $\text{Co}_3\text{O}_4$  and MC, where the porous structure and surface functional groups (Figure S7) of MC may favor the accumulation of reactants through spatial confinement,<sup>[14]</sup> and even favor the formation of intermediates because of the interaction between support and reactants,<sup>[15]</sup> leading to the enhancement of transfer hydrogenation activity over  $\text{Co}_3\text{O}_4$  supported on MC. The synergistic effect is studied in detail in ongoing work. Notably, compared with conventional impregnation methods, where the  $\text{Co}_3\text{O}_4$  particle size distributions are generally very broad, the present synthesis method is simple and generates  $\text{Co}_3\text{O}_4$  nanoparticles with narrow size distribution (ca. 3 nm) and homogeneous dispersion, which allows a highly efficient utilization of Co species on the  $\text{Co}_3\text{O}_4/\text{MC}$ .

The effect of temperature on the transfer hydrogenation reactions was also examined. By increasing the temperature to 140°C and 160°C, the conversions of FAL reached 100% within 3 h and 1 h, respectively (Figure S8a). For HMF to BHMF, the conversions were 100% after reaction for 12 h and 6 h when increasing the temperature to 140°C and 160°C, respectively (Figure S8b). Most importantly, the selectivities towards FOL and BHMF were still higher than 97% in all cases. These results indicate that increasing temperature to 160°C only enhances the reaction rate without affecting the selectivity. For FAL conversion, the reaction rates over  $\text{Co}_3\text{O}_4/\text{MC}$  were calculated. They increase strongly from 37.5 (64% conversion in 2 h), to 148.2 (63% conversion in 0.5 h) and  $401.4 \text{ mmol g}_{\text{Co}_3\text{O}_4}^{-1} \text{ h}^{-1}$  (57% conversion in 0.167 h) by increasing the temperature from 120°C to 140°C, and to 160°C (Table S2, entries 3–5). Also the reaction rates for HMF conversion over  $\text{Co}_3\text{O}_4/\text{MC}$  increase from 11.1 (64% conversion in 6 h), to 57.5 (63% conversion in 1 h) and to  $133.3 \text{ mmol g}_{\text{Co}_3\text{O}_4}^{-1} \text{ h}^{-1}$  (73% conversion in 0.5 h), respectively (Table S2, entries 9–11). These values are one or two orders of magnitude higher than those of  $\text{Co}_3\text{O}_4$ -nanocasting,  $\text{Co}_3\text{O}_4$ -6 nm, and  $\text{Co}_3\text{O}_4$ -17 nm (Table S2, entries 6–8, 12–14). Notably, the activity of  $\text{Co}_3\text{O}_4/\text{MC}$  is comparable to the activities of catalysts for hydrogenation systems involving  $\text{H}_2$ , and higher than activities of other transfer hydrogenation catalysts (Table S3). Moreover, the transfer hydrogenation system using  $\text{Co}_3\text{O}_4/\text{MC}$  as catalyst is much more stable and insensitive to factors (e.g., structure/component of catalysts



and reaction conditions) than the hydrogenation system involving  $H_2$  (Table S3, entries 5–9).

$Co_3O_4/MC$  is also broadly applicable for hydrogenation of other  $\alpha,\beta$ -unsaturated aldehydes. As examples, the conversions of cinnamaldehyde and citral were 99% with selectivities to the corresponding unsaturated alcohols of more than 95% (Figure 3a; Table S2, entries 15 and 16). These unsatu-

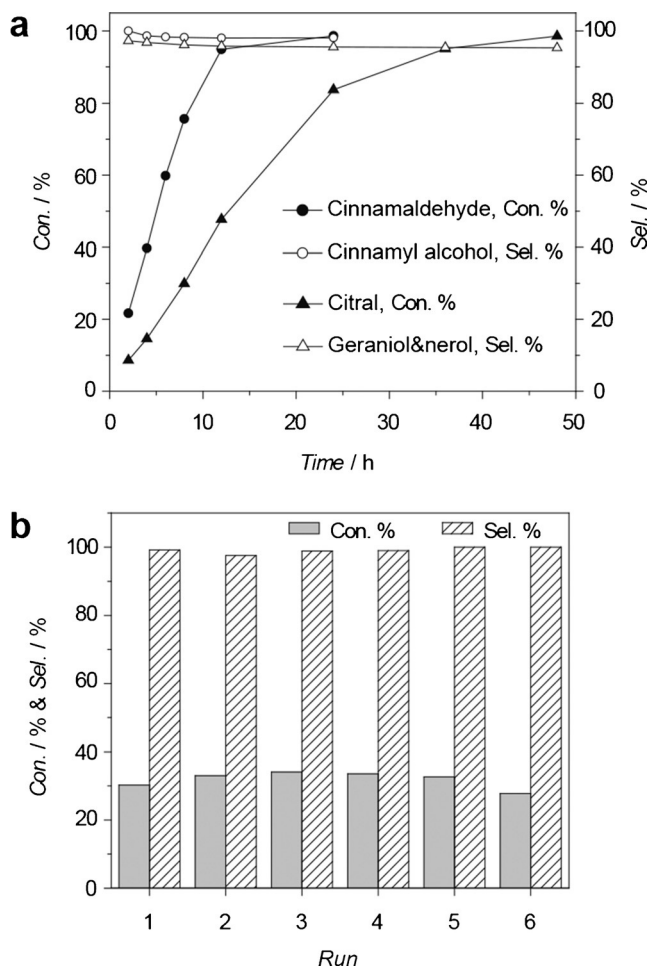


**Figure 3.** a) Catalytic performance in the transfer hydrogenation of cinnamaldehyde and citral over  $Co_3O_4/MC$ . Reaction conditions: 1 mmol substrate, 10 mL 2-propanol, 50 mg  $Co_3O_4/MC$ , 120°C. b) Recycling results for transfer hydrogenation of FAL over  $Co_3O_4/MC$ . Reaction conditions: 1 mmol FAL, 10 mL of 2-propanol, 50 mg  $Co_3O_4/MC$ , 120°C for 1 h.

rated alcohols are industrially important chemical intermediates for production of pharmaceuticals, flavors and cosmetics.<sup>[10b,c]</sup> In addition, never were traces of saturated aldehydes and/or saturated alcohols observed by GC-MS (detection threshold 0.3%). Therefore, the present catalytic system is highly promising for use in industrial production of  $\alpha,\beta$ -unsaturated alcohols.

The reusability of the  $Co_3O_4/MC$  catalyst was investigated using FAL as substrate. For each run, the reaction was carried out at 120°C for only 1 h. The catalyst after reaction was filtrated and washed with 2-propanol, followed by drying and treatment under  $H_2/Ar$  at 300°C for 2 h to remove residues

from the surface of the used  $Co_3O_4/MC$ . In this way, the  $Co_3O_4/MC$  catalyst was recycled at least six times without considerable change in conversion of FAL (the conversions were ranging from 28% to 34% after 1 h), and the selectivity toward FOL was always above 97% (Figure 3b). The TEM images, XRD patterns and  $N_2$  isotherm of  $Co_3O_4/MC$  after six runs (Figure S9) indicate that the mesoporous structure and the particle size of  $Co_3O_4$  were unchanged, confirming the high stability of  $Co_3O_4/MC$  under reaction conditions. In addition, a hot-filtration test was carried out to verify the heterogeneous nature of the reaction. After removal of the solid catalyst, no reaction proceeded in the filtrate (Figure S10). Moreover, no Co species was present in the filtrate (< 0.2 ppm by AAS analysis). These results indicate that the catalytic effect in this system results from the  $Co_3O_4$  nanoparticles and not from leached metal species.

In addition, the transfer hydrogenation process can be easily scaled up since no high pressure (as in hydrogenation with  $H_2$ ) is required. A gram-scale experiment was carried out using 1 mL of FAL (ca. 1.16 g) as substrate at 160°C for 4 h. The conversion of FAL and selectivity for FOL were 100% and > 97%, respectively (Table S2, entry 17). After isolation by rotary evaporation at 80°C under reduced pressure (50 mbar), 1.02 g of FOL (Figure 4a) with purity of approximately 95% was obtained (calculation based on NMR data,

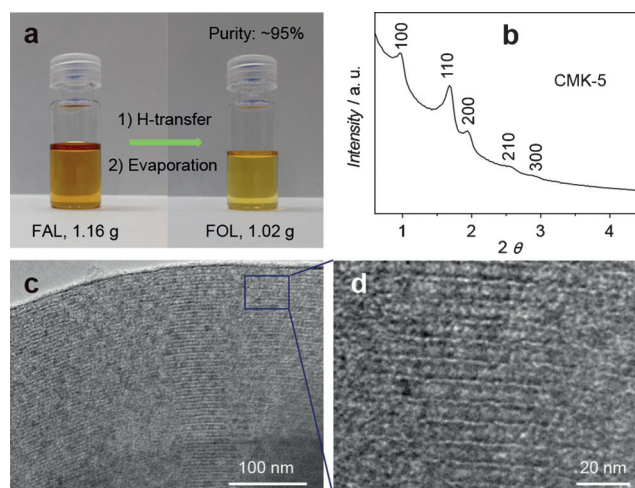


**Figure 4.** a) Photographs of FAL and the product FOL after transfer hydrogenation and evaporation. Reaction conditions: 1.16 g FAL, 100 mL 2-propanol, 500 mg  $Co_3O_4/MC$ , 160°C for 4 h. After isolation by rotary evaporation at 80°C under reduced pressure (50 mbar), 1.02 g of FOL with purity of around 95% was obtained. b–d) XRD pattern and TEM images of CMK-5 using the as-obtained FOL as precursor.

Figure S11). The as-obtained FOL was used as polymer precursor directly without further purification to synthesize ordered mesoporous carbon (CMK-5) via a previously reported method.<sup>[16]</sup> The obtained carbon material possesses the typical highly ordered mesoporous structure (Figure 4b–d).

In conclusion, we have developed a simple and scalable method to synthesize  $Co_3O_4$  nanoparticles supported on the

mesopore framework of the MC. Benefiting from the ion-exchange process, by which cobalt precursor is introduced homogeneously into the polymer framework,  $\text{Co}_3\text{O}_4$  nanoparticles with diameters of around 3 nm are generated which are finely dispersed on the MC framework. The as-obtained  $\text{Co}_3\text{O}_4/\text{MC}$  is an efficient catalyst for transfer hydrogenation of furan-based  $\alpha,\beta$ -unsaturated aldehydes. Selectivities towards unsaturated alcohols are always higher than 95% at full conversion. Furthermore,  $\text{Co}_3\text{O}_4/\text{MC}$  is highly stable under the reaction conditions and can be recycled several times without loss of activity. The gram-scale preparation of FOL over  $\text{Co}_3\text{O}_4/\text{MC}$  indicates that the transfer hydrogenation system is scalable. The as-obtained FOL can be used as polymer precursor directly without further purification to synthesize CMK-5. Thus, the transfer hydrogenation system over  $\text{Co}_3\text{O}_4/\text{MC}$  appears to have potential for applications in industry. In addition, the synthesis route for  $\text{Co}_3\text{O}_4/\text{MC}$ , which is also scalable, can be extended to synthesize other metals or metal oxide catalysts supported on MC.

## Acknowledgements

This work was performed as part of the Clusters of Excellence “TMFB” and “RESOLV”, which are funded by the Excellence Initiative by the German federal and state governments to promote science and research at German universities.

**Keywords:** aldehydes · hydrogen transfer · mesoporous carbon · nanoparticles · supported catalysts

**How to cite:** *Angew. Chem. Int. Ed.* **2016**, 55, 11101–11105  
*Angew. Chem.* **2016**, 128, 11267–11271

- [1] a) J. N. Chheda, G. W. Huber, J. A. Dumesic, *Angew. Chem. Int. Ed.* **2007**, 46, 7164; *Angew. Chem.* **2007**, 119, 7298; b) P. S. Shuttleworth, M. De Bruyn, H. L. Parker, A. J. Hunt, V. L. Budarin, A. S. Matharu, J. H. Clark, *Green Chem.* **2014**, 16, 573; c) C. P. Xu, R. A. D. Arancon, J. Labidi, R. Luque, *Chem. Soc. Rev.* **2014**, 43, 7485; d) P. Gallezot, *Chem. Soc. Rev.* **2012**, 41, 1538; e) A. Corma, S. Iborra, A. Velty, *Chem. Rev.* **2007**, 107, 2411; f) M. Besson, P. Gallezot, C. Pinel, *Chem. Rev.* **2014**, 114, 1827; g) D. M. Alonso, S. G. Wettstein, J. A. Dumesic, *Chem. Soc. Rev.* **2012**, 41, 8075.
- [2] a) J. J. Bozell, G. R. Petersen, *Green Chem.* **2010**, 12, 539; b) R. J. van Putten, J. C. van der Waal, E. de Jong, C. B. Rasrendra, H. J. Heeres, J. G. de Vries, *Chem. Rev.* **2013**, 113, 1499; c) A. A. Rosatella, S. P. Simeonov, R. F. M. Frade, C. A. M. Afonso, *Green Chem.* **2011**, 13, 754; d) S. P. Teong, G. S. Yi, Y. G. Zhang, *Green Chem.* **2014**, 16, 2015; e) K. Yan, G. S. Wu, T. Lafleur, C. Jarvis, *Renewable Sustainable Energy Rev.* **2014**, 38, 663; f) J. A. Melero, J. Iglesias, A. Garcia, *Energy Environ. Sci.* **2012**, 5, 7393.
- [3] a) H. L. Cai, C. Z. Li, A. Q. Wang, T. Zhang, *Catal. Today* **2014**, 234, 59; b) G. H. Wang, J. Hilgert, F. H. Richter, F. Wang, H. J. Bongard, B. Spliethoff, C. Weidenthaler, F. Schüth, *Nat. Mater.* **2014**, 13, 294.
- [4] J. P. Lange, E. van der Heide, J. van Buijtenen, R. Price, *ChemSusChem* **2012**, 5, 150.
- [5] M. S. Ide, B. Hao, M. Neurock, R. J. Davis, *ACS Catal.* **2012**, 2, 671.
- [6] a) B. J. Liu, L. H. Lu, B. C. Wang, T. X. Cai, K. Iwatani, *Appl. Catal. A* **1998**, 171, 117; b) L. Yang, Z. S. Jiang, G. L. Fan, F. Li, *Catal. Sci. Technol.* **2014**, 4, 1123; c) M. Tamura, K. Tokonami, Y. Nakagawa, K. Tomishige, *Chem. Commun.* **2013**, 49, 7034; d) B. S. Takale, S. Q. Wang, X. Zhang, X. J. Feng, X. Q. Yu, T. N. Jin, M. Bao, Y. Yamamoto, *Chem. Commun.* **2014**, 50, 14401.
- [7] a) B. H. Wu, H. Q. Huang, J. Yang, N. F. Zheng, G. Fu, *Angew. Chem. Int. Ed.* **2012**, 51, 3440; *Angew. Chem.* **2012**, 124, 3496; b) I. Cano, A. M. Chapman, A. Urakawa, P. W. N. M. van Leeuwen, *J. Am. Chem. Soc.* **2014**, 136, 2520.
- [8] a) N. Mahata, F. Goncalves, M. F. R. Pereira, J. L. Figueiredo, *Appl. Catal. A* **2008**, 339, 159; b) S. Q. Wei, H. Y. Cui, J. H. Wang, S. P. Zhuo, W. M. Yi, L. H. Wang, Z. H. Li, *Particuology* **2011**, 9, 69; c) C. M. Li, Y. D. Chen, S. T. Zhang, S. M. Xu, J. Y. Zhou, F. Wang, M. Wei, D. G. Evans, X. Duan, *Chem. Mater.* **2013**, 25, 3888; d) Q. Yu, X. Y. Zhang, B. Li, J. Q. Lu, G. S. Hu, A. P. Jia, C. Q. Luo, Q. H. Hong, Y. P. Song, M. F. Luo, *J. Mol. Catal. A* **2014**, 392, 89; e) A. B. Merlo, V. Vetere, J. F. Ruggera, M. L. Casella, *Catal. Commun.* **2009**, 10, 1665; f) K. Fulajtárova, T. Soták, M. Hronec, I. Vávra, E. Dobrocka, M. Omastová, *Appl. Catal. A* **2015**, 502, 78.
- [9] a) J. Kijenski, P. Winiarek, T. Paryczak, A. Lewicki, A. Mikołajski, *Appl. Catal. A* **2002**, 233, 171; b) J. Ohyama, A. Esaki, Y. Yamamoto, S. Arai, A. Satsuma, *RSC Adv.* **2013**, 3, 1033; c) Z. Y. Guo, C. X. Xiao, R. V. Maligal-Ganesh, L. Zhou, T. W. Goh, X. L. Li, D. Tesfagaber, A. Thiel, W. Y. Huang, *ACS Catal.* **2014**, 4, 1340; d) G. Kennedy, L. R. Baker, G. A. Somorjai, *Angew. Chem. Int. Ed.* **2014**, 53, 3405; *Angew. Chem.* **2014**, 126, 3473; e) E. V. Ramos-Fernández, J. Ruiz-Martínez, J. C. Serano-Ruiz, J. Silvestre-Albero, A. Sepúlveda-Escribano, F. Rodríguez-Reinoso, *Appl. Catal. A* **2011**, 402, 50; f) B. F. Machado, S. Morales-Torres, A. F. Perez-Cadenas, F. J. Maldonado-Hodar, F. Carrasco-Marin, A. M. T. Silva, J. L. Figueiredo, J. L. Faria, *Appl. Catal. A* **2012**, 425, 161; g) E. Bailón-García, F. Carrasco-Marin, A. F. Pérez-Cadenas, F. J. Maldonado-Hódar, *Appl. Catal. A* **2014**, 482, 318; h) S. Santiago-Pedro, V. Tamayo-Galvan, T. Viveros-Garcia, *Catal. Today* **2013**, 213, 101; i) P. Concepción, Y. Pérez, J. C. Hernández-Garrido, M. Fajardo, J. J. Calvino, A. Corma, *Phys. Chem. Chem. Phys.* **2013**, 15, 12048; j) S. Bhogswararao, D. Srinivas, *J. Catal.* **2012**, 285, 31.
- [10] a) M. Chatterjee, T. Ishizaka, H. Kawanami, *Green Chem.* **2014**, 16, 4734; b) P. Mäki-Arvela, J. Hájek, T. Salmi, D. Y. Murzin, *Appl. Catal. A* **2005**, 292, 1; c) Y. Yuan, S. Y. Yao, M. N. Wang, S. J. Lou, N. Yan, *Curr. Org. Chem.* **2013**, 17, 400; d) R. Alamillo, M. Tucker, M. Chia, Y. Pagan-Torres, J. Dumesic, *Green Chem.* **2012**, 14, 1413; e) M. J. Taylor, L. J. Durndell, M. A. Isaacs, C. M. A. Parlett, K. Wilson, A. F. Lee, G. Kyriakou, *Appl. Catal. B* **2016**, 180, 580; f) Y. F. Zhu, X. Kong, H. Y. Zheng, G. Q. Ding, Y. L. Zhu, Y. W. Li, *Catal. Sci. Technol.* **2015**, 5, 4208; g) L. L. Yu, L. He, J. Chen, J. W. Zheng, L. M. Ye, H. Q. Lin, Y. Z. Yuan, *ChemCatChem* **2015**, 7, 1701.
- [11] F. Alonso, P. Riente, M. Yus, *Acc. Chem. Res.* **2011**, 44, 379.
- [12] D. Gu, C. J. Jia, C. Weidenthaler, H. J. Bongard, B. Spliethoff, W. Schmidt, F. Schüth, *J. Am. Chem. Soc.* **2015**, 137, 11407.
- [13] Y. M. Dong, K. He, L. Yin, A. M. Zhang, *Nanotechnology* **2007**, 18, 435602.
- [14] a) E. E. Santiso, A. M. George, C. H. Turner, M. K. Kostov, K. E. Gubbins, M. Buongiorno-Nardelli, M. Sliwinski-Bartkowiak, *Appl. Surf. Sci.* **2005**, 252, 766; b) F. Goettmann, C. Sanchez, *J. Mater. Chem.* **2007**, 17, 24.
- [15] a) D. S. Su, J. Zhang, B. Frank, A. Thomas, X. C. Wang, J. Paraknowitsch, R. Schlögl, *ChemSusChem* **2010**, 3, 169; b) J. J. Zhu, J. L. Faria, J. L. Figueiredo, A. Thomas, *Chem. Eur. J.* **2011**, 17, 7112; c) J. L. Figueiredo, M. F. R. Pereira, *Catal. Today* **2010**, 150, 2.
- [16] A. H. Lu, W. C. Li, W. Schmidt, W. Kiefer, F. Schüth, *Carbon* **2004**, 42, 2939.

Received: May 13, 2016

Published online: July 28, 2016